20th Australasian Fluid Mechanics Conference
Perth, Australia
5-8 December 2016

Transient Effects in a Rotating Flapping Wing

W.B. Tay[1], J.W.S. Tay[2] and B.C. Khoo [1,2]

[1]Temasek Laboratories, National University of Singapore, 5A Engineering Drive 1, 117411, Singapore

[2]Department of Mechanical Engineering, National University of Singapore, 9 Engineering Drive 1, 117575, Singapore

Abstract

Transient flows around a rotating, pitching and flapping flat plate have been investigated numerically by varying its flapping frequency, pitching and flapping amplitude. This serves as a canonical problem to flapping micro aerial vehicles (FMAVs) performing turning manoeuvre, with the Re number ranging from 5,000 to 20,000. We solve the simulations using the Immersed Boundary Method (IBM) solver. Changing the frequency has minimal effect on the force output, indicating that the mode of transport is similar across different frequency. Variation of pitching amplitude shows that a higher maximum pitch causes the tip and leading edge vortices to shed early, resulting in the loss of thrust and lift. Lastly, a low flapping amplitude combined with a high pitching amplitude causes a high angle of attack, giving high drag and negative lift. Results obtained from the variation of these parameters allow us to better understand the underlying aerodynamics during the turning manoeuvre of FMAVs.

Introduction

Flapping Micro Air Vehicles (FMAVs) have been gaining interest in recent years, especially in the area of military surveillance, due to their superior manoeuvrability and efficiency at the low Reynolds number regime. In nature, birds and insects can perform tight and sharp turning manoeuvre. However, current FMAVs are still unable to do so, especially at high speed, due to various reasons. Hence, we would like to investigate this problem numerically to obtain a better understanding about the forces and flow field. Due to the complex nature of the problem, we reduce it to a simplified canonical problem, whereby we simulate a flat plate doing a rotation, flapping and pitching motion simultaneously.

Numerical method

The Discrete Forcing Immersed Boundary Method (IBM) [1] approach has been used to solve the 3D non-dimensionalized Navier-Stokes equation. The IBM method uses a non-conforming Cartesian grid, which is especially suited in this case because the plate is constantly moving. In the discrete forcing method, the Navier-Stokes equation is modified by the addition of a forcing term, *fc*, as given by

$$\frac{\partial u}{\partial t} = -u \cdot \nabla u + \frac{1}{\mathrm{Re}} \nabla^2 u - \nabla p + fc \ , \qquad (1)$$

where u, t, p and Re are the velocity vector, time, pressure and the Reynolds number respectively.

The Re is defined as

$$\mathrm{Re} = \frac{Uc}{\upsilon} \ , \qquad (2)$$

where U, c and υ are the reference average plate tip velocity, reference plate chord length and kinematic viscosity of air respectively.

The forces, in non-dimensional terms, based on Kim et al. [2], are calculated as:

$$F_i = -\int_{solid} fc_i^{n+1} dV + \int_{solid} \left(\frac{\partial u_i}{\partial t} + \frac{\partial u_i u_j}{\partial x_j} \right) dV \ , \qquad (3)$$

where V is the volume of the body.

Force calculation and solver validation

In this study, we assume the force coefficients c_t (thrust) and c_l (lift) to be equal to the forces F_i for simplicity. This does not pose any problem because we only compare between results within this study. However, it is also possible to obtain the actual force coefficients or dimensional forces (in Newtons) by multiplying the non-dimensional forces F_i with $2c^2 / S$ or $\rho U^2 c^2$ respectively, where ρ and S are the density of air and the wing planform area respectively.

c_l refers to the force in the vertical y axis direction while c_t refers to the thrust force which is always perpendicular to the length of the wing. This will be more meaningful than using the force in the x or z direction.

The IBM solver has been validated against a 3D plunging wing experiment at Re = 10,000 by Calderon et al. [3] and the hawkmoth / fruit fly model water tunnel experiment by Lua et al. [4]. The reader may refer to the papers by Tay et al. [5] and Tay et al. [6] for part of the validation details.

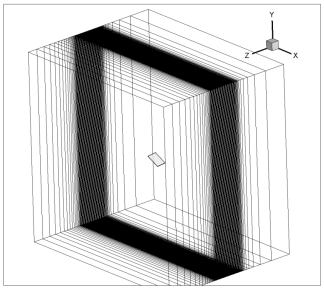

Figure 1. 3D Cartesian grid with flat plate wing.

Simulation setup and grid convergence study

Figure 1 shows the 3D Cartesian grid with the flat plate. The computational domain is 10×10×16.5 in the *x*, *y* and *z*-directions respectively. Grid convergence study shows that a minimum grid length of 0.012*c* is sufficient. Refinement is used in the region near the wings and the resultant total number of cells for the domain is 419×336×481.

The IBM solver has been validated against a 3D plunging wing experiment and successfully used to perform 3D simulations on the Delfly II model [6]. The reader may refer to the paper by Tay et al. [6] for part of the validation details, grid convergence study and application of the IBM solver. The flow is laminar and hence no turbulence models has been added.

Research Methodology

The main objective is to gain a deeper understanding of turning manoeuvre of FMAVs. It is reduced to a simplified canonical problem which involves a flat plate performing rotation, flapping and pitching motion simultaneously. We would like to investigate the effects of flapping frequency, maximum pitch angle θ_{x0} and maximum flapping angle θ_{z0}.

Wing motion

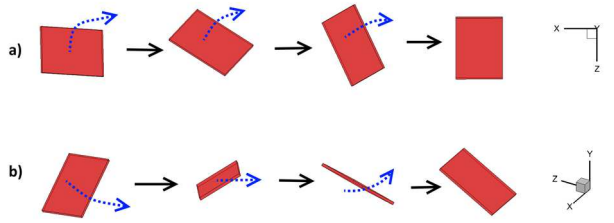

Figure 2. Wing performing rotation + pitching + flapping motion in a) *zx* plane and b) iso plane view. Blue dotted and black arrows indicate direction of motion and subsequent time instants respectively.

The transient simulation involves a flat plate, of aspect ratio 1.5, rotating 90º in quiescent flow. At the same time, the plate pitches up when the wing flaps up (supination) and pitches down as the wing flaps down (pronation). The plate completes one full flap cycle during the 90º rotation. The rotation around the *y* axis undergoes a smoothened impulsive motion from zero to a constant velocity based on the Eldredge function [7] while the pitching (*x* axis) and flapping (*z* axis) undergo sinusoidal motion, shown in Figure 2. Their equations are:

$$\varsigma = \frac{\theta_{y0}}{t_{2e} - t_{1e}}, \tag{4}$$

where $\theta_{y0} = 0.5\pi$, $t_{1e} = 0.5$ and $t_{2e} = 0.725$ respectively. The values are selected such that the plate will rotate 90º in one period.

$$\theta_y = \frac{\varsigma}{2a_e} \ln \frac{\cosh(a_e(t - t_{1e}))}{\cosh(a_e(t - t_{2e}))} + \frac{\theta_{y0}}{2}, \tag{5}$$

where $a_e = 50$ and t = time elapsed respectively.

$$\theta_z = \theta_{z0} \sin(2\pi f_r t - \phi), \tag{6}$$

where $\phi = 0.5\pi$ and f_r = reduced frequency respectively.

$$\theta_x = \theta_{x0} \sin(2\pi f_r t) \tag{7}$$

$$f_r = \frac{fc}{U}, \tag{8}$$

where f = flapping frequency.

Simulation parameters

There are 3 parameters to be investigated. They are flapping frequency f (10 – 40Hz, 10Hz interval), pitch amplitude θ_{x0} (20 to 50º, 10º interval) and flapping amplitude θ_{z0} (10 to 40º, 10º interval). These 3 parameters are chosen as they are important factors when a wing perform transient rotation.

Our FMAVs of interest has a wingspan of approximately 15cm. Using this value as a starting point, we get a chord length of 5cm. For example, with $\theta_{z0} = 30º$, f = 10Hz, Re ~ 5,000.

Simulation cases

We separate the simulations into 3 parts. In the first part (A), the focus is on the effect of flapping frequency. In the second and third part (B,C), we focus on the effects of pitching amplitude angle θ_{x0} and flapping amplitude θ_{z0} variation respectively. The simulation cases are:

Case	θ_{x0} (º)	θ_{z0} (º)	f (Hz)	Re
A1 - 6	40	30	1 – 40	500 – 20,000
B1 - 4	20 – 50	30	30	15,000
C1 - 4	40	10 - 40	30	5,000 – 20,000

Table 1. Simulation parameters for frequency, θ_{x0} and θ_{z0} variation.

Results and Discussions

Effect of Flapping Frequency

The flapping frequency varies from 10 to 40Hz. According to the definition of Re, this gives Re ranging from 5,000 to 20,000. From Figure 3, we observe from the force results that there is almost no difference across the different Re. This prompt us to do additional cases at Re = 500 and 1,000 (equivalent to frequency of 1 and 2Hz respectively), which showed slight difference. This indicates that in these simulations, the mode of transport is very similar. The slight difference is due to the effect of viscous force, which is much weaker at Re > 5,000.

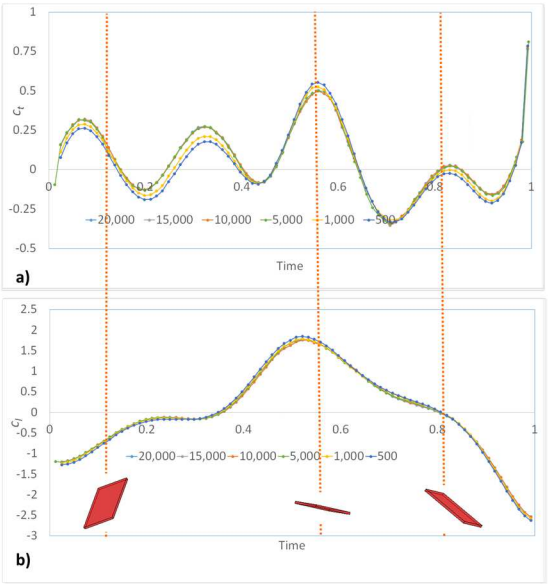

Figure 3. a) c_t and b) c_l of cases A1-6 over one period. The red dotted lines correspond to the time instants in Figure 5. The red plate indicates its position at its current instant.

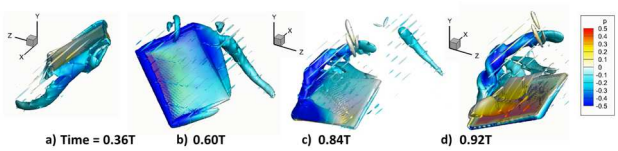

Figure 4. Q criterion = 10 of case A1 with pressure contours at different instants in time.

We now analyse the flow evolution as the wing pitches, flaps and rotates. We choose to present the Re = 500 case (A1) because the formation and evolution of the flow structures are insensitive to the Re. At Re > 5,000, there is a larger range of length scales, resulting in discontinuous iso-surface visualizations of the coherent structures in the flow [8]. Figure 4 shows the Q criterion iso-surface with pressure contours of the plate at different instants in time. After a short while from rest, a tip vortex (TV) can be observed due to the higher plate tip velocity. At time = 0.36T, the tip vortex begins to shed while still being attached to the plate's tip. At time = 0.60T, the tip vortex has shed and the leading (LEV), trailing (TEV) edge vortices have started to grow in size due to the increased velocity. At time = 0.84T, the TEV has shed and a new TV is formed again. Meanwhile, the LEV remains attached and keeps growing. Throughout this interval, the pressure contours show that pressure on the topside of the plate remains low. Finally, at time = 0.92T, the LEV sheds and there is a recovery of pressure, evident from the change in pressure contour colour from blue to red.

Now, we return to analyse the variation of force during the transient period. Figure 3 and Figure 5 show the c_t / c_l of cases A1-6 over one period and the pressure iso-surface at radius 1.5c from the rotation center respectively. The variation of forces over the transient period is mainly due to the pressure distribution on the top and bottom surface of the plate and its angle orientation. At time = 0.12T, c_l is negative because pressure is higher on the plate's top compared to its bottom. The angle of attack of the plate is also low, and the projection of force gives a small amount of thrust. At time = 0.56T, low pressure is now on the plate's top, which resulted in high values of lift. Similarly, the wing is in its pronation stage, giving high c_t at the same time. Lastly, at time = 0.80T, low pressure difference between the plate's top and bottom gives almost zero thrust and a small amount of lifts.

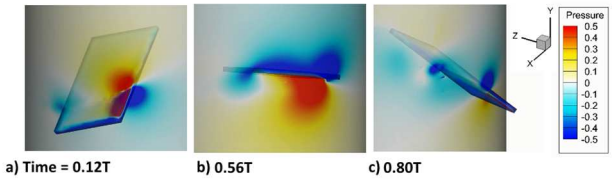

Figure 5. Pressure iso-surface at radius 1.5c from rotation centre.

Effect of Maximum Pitch Angle θ_{x0}

In this section, θ_{x0} varies from 20° to 50°. θ_{z0} remains at 30° and hence the Re for all cases B1-4 are 15,000. For ease of comparison, we select two cases (B1, 20° and B4, 50°) to illustrate the differences. The force graphs and pressure iso-surface are given in Figure 7 and Figure 8 respectively. At time = 0.2T, c_t for B1 is positive but it is negative for B4. If we look at the surface pressure of the plates on these two cases, we observe that pressure is high / low on the top / bottom surface of the plate for B1 but reversed for B4. Hence, due to force vectoring, thrust and drag are experienced for the plate in B1 and B4 respectively. The same principle applied to the thrust and lift at time = 0.52T and 0.80T. Interestingly, higher pitch angle does not translate into higher thrust or lift. As shown in Table 2, B1 has the highest thrust and lift but B4 develops drag and its lift is low. This is because for B4, the high velocity at the plate's tip cause the TV and LEV to shed early, reducing the thrust and lift. This indicates that when FMAV executes turning manoeuvre, the pitch angle may need to be changed to reduce drag.

Case	B1	B2	B3	B4
Average c_t	0.19	0.15	0.07	-0.03
Average c_l	0.09	0.03	0.02	0.03

Table 2. Average c_t and c_l for case B1-4.

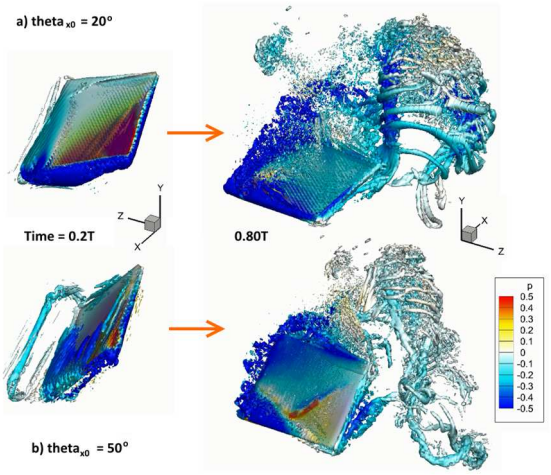

Figure 6. Q criterion = 10 iso-surface for θ_{x0} = a) 20° and b) 50° at two instants in time.

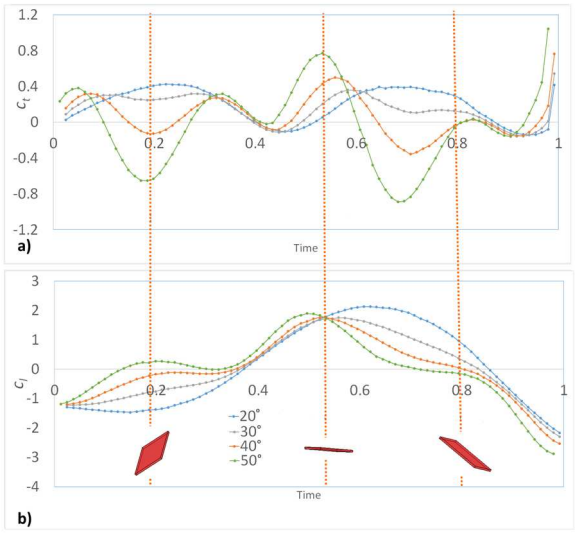

Figure 7. a) c_t and b) c_l of cases B1-4 over one period. The red dotted lines correspond to the time instants in Figure 8.

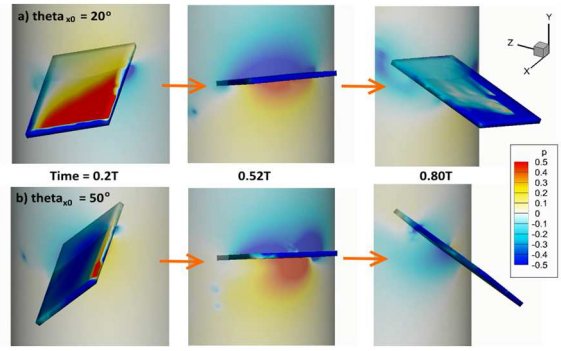

Figure 8. Pressure iso-surface at radius 1.5c for θ_{x0} = a) 20° and b) 50°.

Effect of Maximum Flapping Angle θ_{z0}

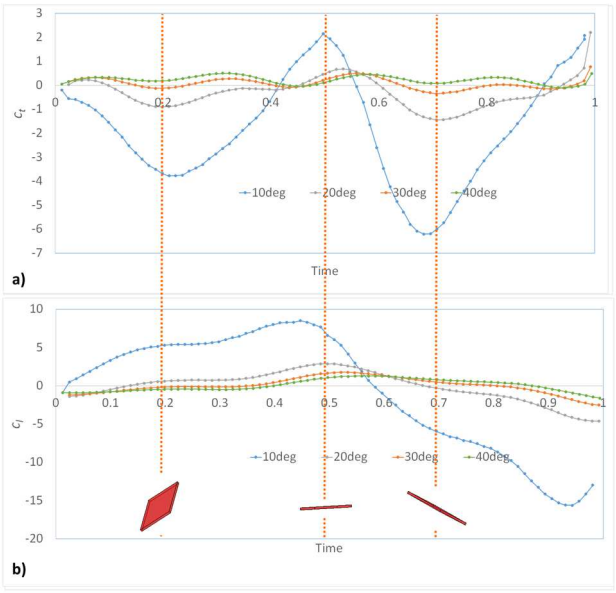

Figure 9. a) c_t and b) c_l of cases C1-4 over one period. The red dotted lines correspond to the time instants in Figure 10.

We investigate the effect of flapping amplitude θ_{z0} in this section. Because the tip velocity depends on θ_{z0}, the Re and f_r both change as θ_{z0} changes, as shown in Table 3. Figure 9 and Figure 10 show the c_t / c_l of cases C1-4 over one period and pressure iso-surface at radius 1.5c for θ_{z0} = 10° / 40° respectively. Comparing between C1 (θ_{z0} = 10°) and C4 (θ_{z0} = 40°), due to the high f_r for C1, its magnitude is much larger than that of C4. For C1, upward motion is small with respect to θ_{x0}. At time = 0.2T, this high angle of attack gives high lift and drag at the same time. We can also observe the large pressure difference in Figure 10. The pressure is very low on the plate's top. This result is similar to the study on rotating-pitching plates by Percin and van Oudheusden [9]. The same reasoning applies during the downstroke at time = 0.7T. For C4, its θ_{x0} is 40° which gives a very different incoming relatively velocity, as compared to C1. Moreover, the f_r for C4 is lower than that of C1. The average c_t / c_l for C1 and C4 are -1.60 / -0.80 and 0.10 / 0.03 respectively. Hence, if an FMAV undergoes a turning manoeuvre, the large drag and negative lift will be very unfavourable for the FMAV.

Case	θ_{z0} (°)	f_r	Re	Average c_t	Average c_l
C1	10	0.955	5,000	-1.83	-0.80
C2	20	0.477	10,000	-0.31	-0.06
C3	30	0.318	15,000	0.07	0.02
C4	40	0.239	20,000	0.22	0.03

Table 3. Parameters for C1-4.

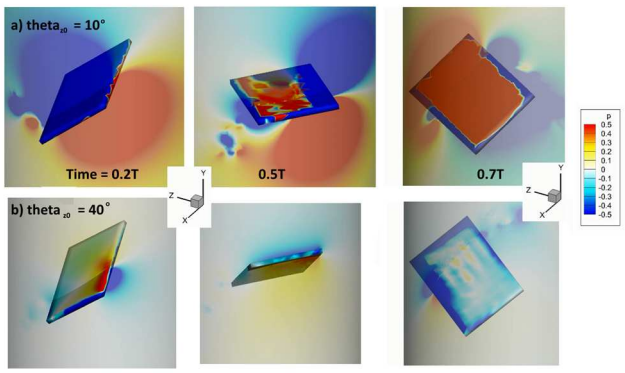

Figure 10. Pressure iso-surface at radius 1.5c for θ_{z0} = a) 10° and b) 40°.

Conclusions

Simulations have been performed on the transient motion of plate undergoing rotation pitching and flapping motion. Results show that changing the flapping frequency has minimal effect on the c_t and c_l, indicating the mode of transport is the same across different frequency. Increasing the pitch amplitude θ_{x0} does not translate into higher lift and thrust. This is because the high velocity at the plate's tip cause the TV and LEV to shed early, reducing the forces. Lastly, a low flapping amplitude θ_{z0} in the current scenario is detrimental during an FMAV's turning manoeuvre because it creates high drag and negative lift during the transient motion. These results will serve as important considerations when FMAVs perform turning manoeuvre.

Acknowledgments

The computational work for this article was partially done on resources of the National Supercomputing Centre, Singapore (https://www.nscc.sg).

References

[1] Bandringa, H., Immersed boundary methods, University of Groningen, 2010.

[2] Kim, J., Kim, D., and Choi, H., An immersed-boundary finite-volume method for simulations of flow in complex geometries, *Journal of Computational Physics*, **171**, 2001, 132–150.

[3] Calderon, D.E., Wang, Z., and Gursul, I., Lift enhancement of a rectangular wing undergoing a small amplitude plunging motion, in *48th AIAA Aerospace Sciences Meeting*, 2010.

[4] Lua, K.B., Lim, T.T., and Yeo, K.S., Scaling of Aerodynamic Forces of Three-Dimensional Flapping Wings, *AIAA Journal*, **52**, 2014, 1095–1101.

[5] Tay, W.B., Oudheusden, B.W. van, and Bijl, H., Numerical simulation of X-wing type biplane flapping wings in 3D using the immersed boundary method, *Bioinspiration & biomimetics*, **9**, 2014, 036001.

[6] Tay, W.B., Deng, S., Oudheusden, B.W. van, and Bijl, H., Validation of immersed boundary method for the numerical simulation of flapping wing flight, *Computers & Fluids*, **115**, 2015, 226–242.

[7] Eldredge, J.D., Wang, C., and OL, M. V., A Computational Study of a Canonical Pitch-up, Pitch-down Wing Maneuver, in *39th AIAA Fluid Dynamics Conference*, 2009.

[8] Viswanath, K., Nagendra, K., Cotter, J., Frauenthal, M., and Tafti, D.K., Straight-line climbing flight aerodynamics of a fruit bat, *Physics of Fluids*, **26**, 2014, 1–28.

[9] Percin, M. and Oudheusden, B.W. van, Three-dimensional flow structures and unsteady forces on pitching and surging revolving flat plates, *Exp Fluids*, **56**, 2015, 1–19.